IEEE Photonics Journal
An IEEE Photonics Society Publication

Open Access

990 nm High-Power High-Beam-Quality DFB Laser With Narrow Linewidth Controlled by Gain-Coupled Effect

Volume 11, Number 1, February 2019

Yu-Xin Lei
Yong-Yi Chen
Feng Gao
De-Zheng Ma
Peng Jia
Qiu Cheng
Hao Wu
Chun-Kao Ruan
Lei Liang
Chao Chen
Jun Zhang
Jing-Yu Tian
Li Qin
Yong-Qiang Ning
Li-Jun Wang

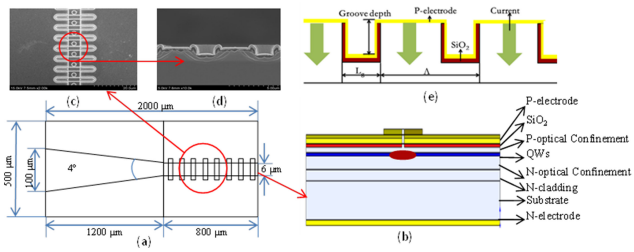

DOI: 10.1109/JPHOT.2019.2893961
1943-0655

990 nm High-Power High-Beam-Quality DFB Laser With Narrow Linewidth Controlled by Gain-Coupled Effect

Yu-Xin Lei,[1, 2] **Yong-Yi Chen**,[1] **Feng Gao**,[1, 2] **De-Zheng Ma**,[1, 2] **Peng Jia**,[1] **Qiu Cheng**,[1, 2] **Hao Wu**,[1] **Chun-Kao Ruan**,[1, 2] **Lei Liang**,[1] **Chao Chen**,[1] **Jun Zhang**,[1] **Jing-Yu Tian**,[1, 2] **Li Qin**,[1] **Yong-Qiang Ning**,[1] **and Li-Jun Wang**[1]

[1]State Key Laboratory of Luminescence and Application, Changchun Institute of Optics, Fine Mechanics and Physics, Chinese Academy of Sciences, Changchun 130033, China
[2]Daheng College, University of Chinese Academy of Sciences, Beijing 100049, China

DOI:10.1109/JPHOT.2019.2893961

Manuscript received December 12, 2018; revised January 11, 2019; accepted January 15, 2019. Date of publication January 18, 2019; date of current version February 8, 2019. This work was supported in part by the National Science and Technology Major Project of China under Grant 2016YFE0126800, in part by the Frontier Science Key Program of the President of the Chinese Academy of Sciences under Grant QYZDY-SSW-JSC006; in part by the National Natural Science Foundation of China under Grants 11874353, 61727822, 61674148, 11604328, 51672264, 61474117, and 61874119; in part by the Natural Science Foundation of Jilin Province (Jilin Province Natural Science Foundation) under Grants 20160520017JH and 20170623024TC; in part by the Science and Technology Key Project of Jilin Province under Grant 20170204013GX; in part by the Science and Technology Development Project of Jilin Province under Grant 20180201014GX; and in part by the Opened Fund of the State Key Laboratory of Integrated Optoelectronics under Grant IOSKL2018KF21. Corresponding authors: Yong-Yi Chen, Feng Gao, and Peng Jia (e-mail: chenyy@ciomp.ac.cn; summit1990@163.com; jiapeng@ciomp.ac.cn).

Abstract: High-power single-longitudinal-mode regrowth-free gain-coupled distributed feedback laser diode based on ridge waveguide with periodic current injection is achieved at 990 nm. Our device is fabricated only by standard i-line lithography with micron-scale precision, obtains an excellent performance at high injection current. A continuous-wave power of over 0.681 W is achieved at 3 A. The maximum continuous-wave power at single-longitudinal-mode operation is up to 0.303 W at 1.4 A. Narrow linewidth emission has been reached with a 3 dB spectrum width less than 1.41 pm. The high side mode suppression ratio is over 35 dB. The lateral far field divergence angle is only 15.05°, the beam quality factor M^2 is 1.245, achieving a laterally near-diffraction-limit emission. It is more beneficial for single-mode fiber coupling as pumping sources and other applications which require high beam quality at high power with easy fabrication technique.

Index Terms: Semiconductor lasers, gain-coupled DFB, single-longitudinal mode, narrow linewidth.

1. Introduction

Distributed feedback (DFB) semiconductor lasers with single-longitudinal-mode (SLM) operation and narrow linewidth [1], [2] are widely used in a variety of applications such as telecommunication systems [3], materials processing [4], scanning [5], medicine [6], light detection and ranging (LIDAR) [7]–[9], pumping sources for Er-doped fiber amplifier (EDFA) [10] and fiber optic gyroscope [11]. Ordinary gain-coupled DFB lasers based on periodic gain (or loss) and index-coupled DFB

lasers with periodically changed refractive index suffer from different problems [12] due to their different structural characteristics as discussed in [13]. Solutions [14]–[18] to these problems are often accompanied by high-cost and time consuming complex fabrication technique [19] such as complicated epitaxial regrowth technology or delicate nanometer-scale gratings fabrication technology [20]. Meanwhile, DFB lasers with mode-selection gratings filtering unwanted lasing modes often result in low power [21]. Traditional master oscillator power amplifier (MOPA) structure is usually introduced to amplify the output power without beam quality degeneration [22]. The large output aperture of the MOPA device leads to the poor near field and far field performances. The large far field divergence angle and the large-size near field optical spot enhance the difficulty and the complexity of beam shaping and coupling.

In this paper, a low-cost regrowth-free gain-coupled DFB laser with a tapered waveguide is proposed. The gain-coupled DFB laser device realizes enhanced output power, high side mode suppression ratio (SMSR), SLM stabilization, narrow linewidth, and laterally near-diffraction-limit emission simultaneously. The structure, which consists of a ridge waveguide at front and a tapered waveguide at back, is introduced to improve the output power of the device with SLM emission. Gain-coupled effect is caused by periodic current injection from periodic surface metal p-contacts insulated by periodic shallow-etched grooves. Gain contrast in quantum wells is formed without effective index-coupled effect, thus the loss introduced by index contrast is minimized. Meanwhile, 2 μm-width shallow-etched grooves, fabricated only by ordinary i-line lithography, simplify the difficulty of fabrication without using complex fabrication steps, such as expensive and time-consuming epitaxy regrowth or nanometer-scale grating fabrication technology. Moreover, the excellent performance and stable operation are still achieved under the simple and low-cost technology. The enhanced high continuous-wave (CW) output power reaches up to 0.681 W at 3 A, which is much larger than the reported gain-coupled DFB lasers [24]. The slope efficiency is over 0.27 W/A, twice larger than 0.11 W/A of the previously reported gain-coupled DFB lasers [25]. Stable and high SLM CW output power reaches up to 0.303 W at 1.4 A, much larger than reported high power SLM lasers [1]. High SMSR of 35 dB is larger than diode lasers with nanometer-scale gratings [26]. Narrow 3 dB linewidth is 1.41 pm, much narrower than lasers with surface high-order gratings [2]. The far field divergence angle in slow axis is 15.05°, a laterally near-diffraction-limit emission is achieved with the beam quality factor M^2 in the slow axis of 1.245, much better than previously reported SLM DFB lasers [27]. The excellent beam quality reduces the difficulty of coupling and shaping. Hence, our gain-coupled DFB laser provides an effective method to realize high-power, near-diffraction-limit, SLM lasers. The low cost and simplified fabrication technique enhance its potential for widespread commercial applications. And it allows the design of high-power high-beam-quality laser systems with simple beam coupling and shaping systems.

In the following sections, we presents the design process and performance of our device. First, a brief overview of the device structure is given. Second, details of design and fabrication are presented. Finally, the testing results regarding electro-optical, spectral and spatial properties of our device are provided.

2. Structure and Fabrication

As shown in Fig. 1(a), our device consists of an 800 μm-long 6 μm-wide ridge waveguide at front and a 1200 μm-long tapered waveguide with a full angle of 4°. The epitaxial layer structure of our device bases on a self-designed ultra-low-aluminum asymmetrical ultra-large-optical-cavity (ULOC) wide-waveguide structure [28], including an asymmetric separate confinement heterostructure (SCH) with double strain-compensated InGaAs quantum wells as shown in Fig. 1(b). The thicknesses and compositions of AlGaAs waveguides and cladding layers were well designed to achieve high power, low far field divergence angle, and high threshold of catastrophic optical damage (COD).

The parameters of the ridge waveguide and the tapered waveguide in our 2 mm-cavity-length gain-coupled DFB laser are carefully designed in consideration of the combination of theory and experimental conditions. The ridge waveguide listed at front is utilized to obtain fundamental transverse mode and SLM operation simultaneously. The width and etching depth of the ridge waveguide

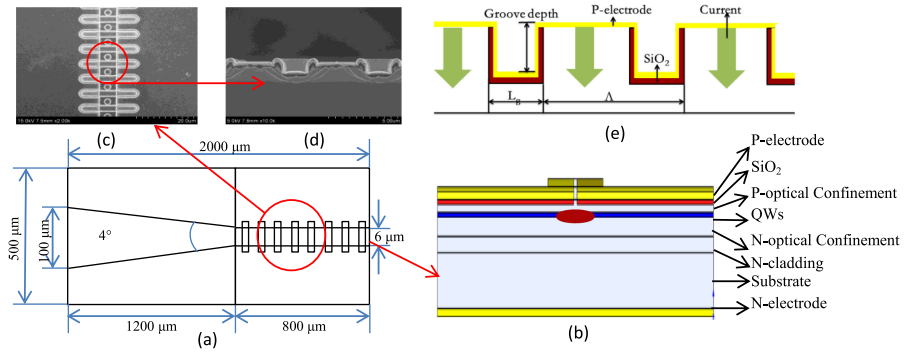

Fig. 1. (a) Layout of the gain-coupled DFB laser with surface-etched grooves. (b) Epitaxial layer structure. (c) The scanning electron microscope image of the periodic surface electrodes from top view. (d) The scanning electron microscope image of the periodic surface etched grooves from lateral view. (e) Periodic current injection schematic.

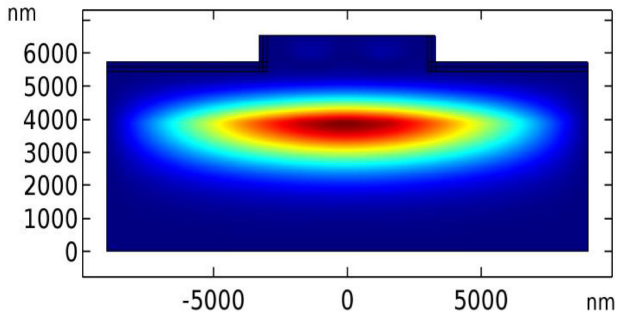

Fig. 2. The normalized electrical field distribution of the ridge waveguide with the width of 6 μm and etching depth of 1 μm.

are derived from the single mode conditions for three layers slab waveguide [29], and are finally set to be 6 μm and 1 μm. Fundamental transverse mode operation is achieved as the normalized electrical field distribution calculated by the commercial software COMSOL Multiphysics shown in Fig. 2. SLM narrowband emission is obtained from an additional wavelength selective feedback by implementing gain-coupled DFB gratings on the ridge waveguide. As the schematic of our device shown in Fig. 1(e), the gain-coupled mechanism is formed by periodic current injection from periodic surface metal p-contacts and insulated periodic shallow-etched surface grooves filled with silica. According to our previous research [13], the insulated grooves can effectively increase the gain contrast in the quantum wells. The coupling coefficient κ demonstrating the strength of gain coupling mechanism is $\kappa = i\frac{\Delta g\Gamma}{4}$, where Γ is the optical confinement factor in the quantum wells, Δg is the gain/loss contrast in the waveguide. For κ is independent of grating period, we use high-order insulated surface grooves to achieve gain-coupled mechanism and reduce processing difficulty. As the scanning electron microscope (SEM) image shown in Fig. 1(d), the groove is shaped as rectangle with a length of 2 μm, which is compatible with our alignment technology of the top contact in fabrication. The 44^{th} order surface gain-coupled grating with a large period is chosen to realize micrometer-scale periodic grooves which are much easier to fabricate by standard i-lithography than nanometer-scale gratings or apodized gratings [17]. The residual layer thickness, from the bottom of the surface grooves to the quantum wells, has been exactly designed to enhance the gain contrast in quantum wells without introducing effective index-coupled effect, and is finally determined as 1.1μm to realize large κ with small total loss. As shown in Fig. 1(c), the width of the grooves is 20 μm, which is larger than the width of ridge waveguide. The excess parts of the grooves aside the ridge serve as isolation etched grooves which filter high order transverse modes reflected from

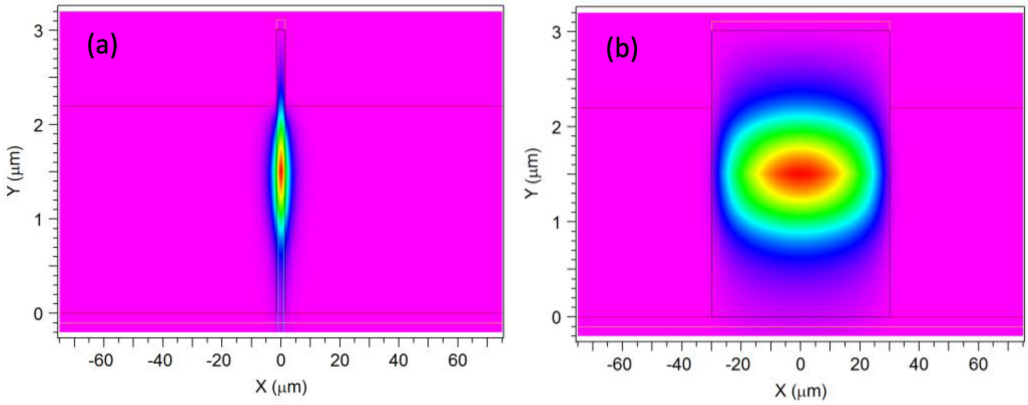

Fig. 3. Transverse field profile (a) at ridge side's facet, (b) at tapered side's facet.

the rear facet, and are just simultaneously formed with the gain-coupled grooves without further more steps.

The tapered waveguide is introduced to enhance the output power due to its large surface for current injection, just like the amplifier section of the MOPA structure [22]. Most tapered waveguides in MOPA structures are gain-guided for obtaining the homogeneity of the light field on the output facet, but sacrificing the restriction of the light field [30]. The tapered waveguide of our device is index-guided, which can provide more effective restriction of the light while no effect on the output facet. What's more, the index-guided tapered waveguide effectively simplifies the process of the fabrication by being formed simultaneously with the ridge waveguide. The full angle of the tapered waveguide, which is less than the angle of fundamental mode diffraction, is set to be 4°. Different from traditional MOPA structure, the tapered waveguide of our device is set at back of the ridge waveguide. As the normalized transverse electrical field distributions calculated by BeamProp software shown in Fig. 3, the aperture width of ridge side's facet is much narrower than tapered side's facet, our device provides obvious advantages and potentials when the coupling and shaping are required. The width of the tapered waveguide ranges from 6 μm to 100 μm as the length is 1200 μm for enough optical amplification. And the high-order transverse modes suffer from more scattering loss than fundamental transverse mode. The COD threshold of the rear facet is effectively improved by significantly reducing the power density [31]. Though the front facet is relatively narrow, it's still wider than the ridge side's facet of ordinary MOPA laser [22], carefully designed ULOC waveguide broadens the mode distribution and maintains fundamental mode lasing, meanwhile grooves aside the ridge helps to scatter high order modes and other reflection modes from the tapered amplifier. Then the COD threshold of the whole device is improved.

The epitaxial layer structure of our device was grown by metal organic chemical vapor deposition (MOCVD) on a GaAs substrate. The periodic shallow-etched grooves, the lateral waveguides, and the periodic surface metal p-electrodes were patterned in turn after epitaxial material growth. Due to the micrometer-scale of the structure, the device was precisely defined and formed by standard i-line lithography and ordinary inductively coupled plasma (ICP) etching techniques with high stability and reproducibility. The i-line lithography with low costs and simplified manufacturing process is more practical and applicable in actual production than electron-beam lithography. Etched SiO_2 on top of the ridge waveguide (see Fig. 1(d) and Fig. 1(e)) separated by isolated grooves act as current injection windows and then covered by metal. After electroplating with gold and metallization, the wafer was cleaved into bars with a cavity length of 2 mm. The laser bars were then cleaved into 500 μm-wide single emitters after coating with anti-reflectivity (AR) / high-reflectivity (HR) films on front/rear facets, respectively. Single emitters were mounted p-side down on AlN sub-mounts with hard solder. Golden wire bonds were used to contact the n-side with the sub-mounts for electric connection in CW measurement. Then, the chips on sub-mounts were mounted on copper heat sinks for water-cooling in further testing and analysis.

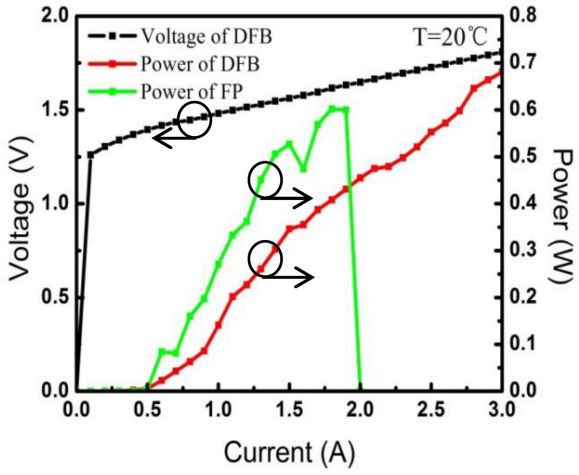

Fig. 4. Power–current–voltage characteristics profiles of DFB laser and FP laser.

Thus, our gain-coupled DFB laser device provides higher SLM output power than the narrow tripe SLM laser [24], narrower aperture width, which makes it easy for coupling and shaping, than high output power laser with MOPA structure [23], and easier fabrication technique than traditional DFB laser [20].

3. Results and Discussion

All measurements were carried out under continuous wave (CW) conditions at a heat sink temperature of $T_{HS} = 20$ °C. All devices for comparisons were fabricated simultaneously on the same wafer. The optical output power was measured with a thermoelectric detector, which was calibrated as national standards, placed directly in front of the output facet. The spectrum characterization was measured by directly coupling the laser with a 10 μm core diameter fiber-linking YOKOGAWA AQ6370C optical spectrum analyzer. The linewidth was measured by coupling the collimated laser to Fabry–Perot Interferometer (Thorlabs, SA200-8B) with the resolution of 67 MHz and the free spectral range of 10 GHz.

The power–current–voltage (PIV) characteristic profiles of the 2 mm-cavity-length gain-coupled DFB laser are shown in Fig. 4. The output power of the DFB device reaches up to 0.681 W at 3 A. It is much larger than reported gain-coupled DFB lasers [24]. The threshold current is measured to be 500 mA and the slope efficiencies is over 0.27 W/A, which is more than twice larger than 0.11 W/A of the gain-coupled DFB laser with a titanium surface Bragg grating [25]. The power–current (PI) characteristic of the Fabry-Perot (FP) device only without surface etched grooves is also depicted in Fig. 4 for comparison. Because the gain-coupled mechanism and lateral grooves filters unwanted wavelengths and high order modes [26], the slope efficiency and the output power of the gain-coupled DFB device are both inferior to the FP device. The output power of the gain-coupled DFB device increases linearly in the whole test range without kink, roll-over or COD. The reference PI profile of FP device shows a kink at a current around 1.6 A, the slop efficiency decreases at higher currents and sharply drops down at 2 A.

As shown in Fig. 5(a), SLM operation is achieved with wavelength stabilization at a large range of current from threshold to 1.4 A. The maximum output power in SLM operation is 0.303 W at around 990 nm. The maximum SMSR is over 35 dB as shown in Fig. 5(b), which is higher than reported single-mode laser [26]. As the inset of the Fig. 5(a) shows, the value of SMSR goes up first and then down, and reaches the maximum value at 0.8 A. In low current form threshold to 0.8 A, the DFB section dominates in the longitudinal mode operation, working as master oscillator pumping the taper section where has a low gain in low current. The wavelength selection ability of the DFB section increases with the current. When the current increases beyond 0.8 A, the power in the tapered

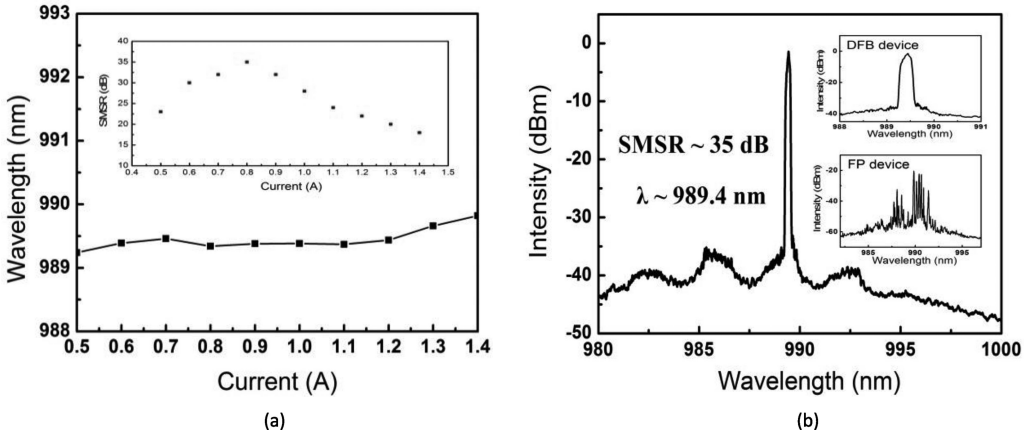

Fig. 5. (a) Wavelength with various currents at 20°C. The inset shows the SMSR information. (b) The optical spectrum at 0.8 A with a SMSR of 35 dB. The insets show the zoomed in optical spectrum of the DFB device and the optical spectrum of the reference FP device at 0.8 A.

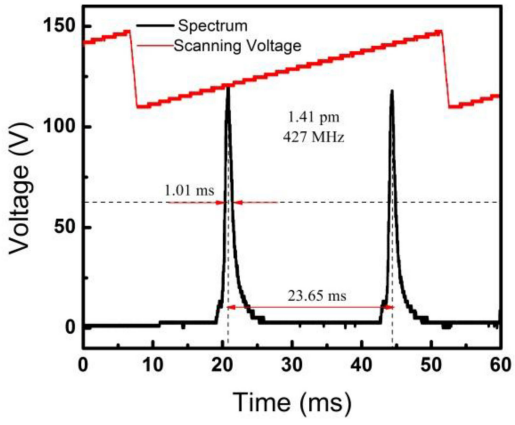

Fig. 6. The linewidth pattern of the gain-coupled DFB device at 1 A.

section increases dramatically rather than the DFB section. The multi-longitudinal modes in tapered waveguide also increase intensely as the current increases. The back reflection of the tapered section tends to decrease the SMSR due to the mode competition at high current. In a large range of current our device behaves single frequency characteristic. The ridge waveguide output facet can increase the coupling efficiency to fibers. Even though the fluctuation existed, our device can reach a much high pumping efficiency for pumping EDFA or fiber lasers thanks to its wavelength stability and SLM property. As shown in Fig. 6, the 3 dB spectral linewidth of the narrowband emission is only 1.41 pm (427 MHz) which is calculated from $(1.01\,\text{ms} / 23.65\,\text{ms}) * 10\,\text{GHz} = 427\,\text{MHz}$ and $427\,\text{MHz} * \lambda^2/c = 1.41\,\text{pm}$, the 3 dB spectral linewidth of our device is much better than the reported DFB laser with the linewidth of 10 pm [2]. The zoomed in optical spectrum of the DFB laser device and optical spectrum of the FP laser device are shown in the insets of the Fig. 5(b). The spectrum of the FP reference device shows a main lobe and several side lobes, each lobe contains multiple peaks corresponding to multiple longitudinal modes. The observed multiple-longitudinal-mode operation is potentially caused by the multiple modes occurred in tapered waveguide at high injection currents [23], and the rising heat accumulations within the device is the main reason for the reduction in the electro-optical efficiency, and the roll-over phenomenon. The wavelength stabilization in SLM operation is attractive in pumping EDFAs [10] or fiber optic gyroscope [11]. The gain-coupled ridge

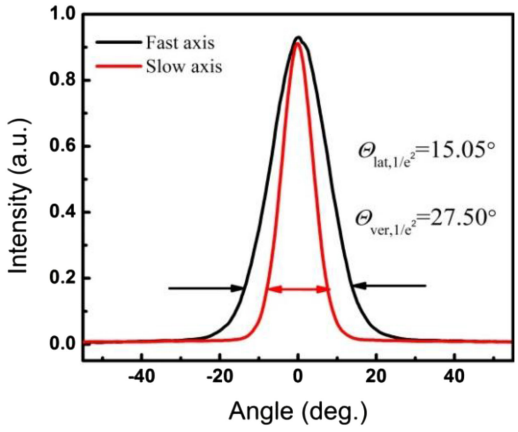

Fig. 7. Normalized intensity distribution of the far field patterns.

waveguide has a smaller current injection surface thus larger resistance and higher working voltage thanks to etched grooves, and current injection has a distribution between the tapered waveguide and the gain-coupled ridge waveguide when they are parallel connected to each other in our p-side down mounting. It is more prone that current inject to the tapered waveguide. As the current in the gain-coupled ridge waveguide almost maintains the same, the temperature seldom changes and the wavelength maintains stable in quite a wide range of 0.9 A.

The lateral and vertical divergence characteristics of the gain-coupled DFB laser are obtained from measurements at 2 A and are depicted in Fig. 7. The profiles of far field are individually normalized in intensity of 1. Far-field patterns keep on-axis main-lobe near Gaussian distribution over the entire tuning range with minor changes in shape and width. The vertical beam divergence angle at $1/e^2$ is 27.5°, benefitting from the implementation of an asymmetric large optical cavity structure with the active layer positioned not in the middle of the waveguide layers but closer to the p-side. The lateral beam divergence angle at $1/e^2$ is 15.05°. The value of the beam propagation factors M^2 in slow axis is only 1.245, which is much better than previous SLM DFB lasers [27], indicating a fundamental transverse mode lasing. Owing to the narrow width of the ridge waveguide, our device achieves a near-diffraction-limit emission along the lateral direction, which makes it suitable for coupling or shaping.

The gain-coupled DFB ridge based on periodic current injection is the crucial part in our device. First, it provides gain coupled mechanism to realize SLM operation with an easy processing procedure. Second, thanks to higher electrical resistance caused by smaller current injection area, this part also helps stabilize the lasing wavelength in a wide current range from 0.5 A to 1.4 A. Third, it maintains single mode lasing with an excellent beam quality even at high output power, and the narrow ridge lasing facet is suitable for single mode fiber coupling, making it useful as pumping sources for fiber components. Fourth, the shallow-etched grooves aside the ridge waveguide provide more scattering loss for high-order modes than the fundamental mode; they also provide scattering loss to slab modes caused by the back reflections from the taper waveguide, which helps maintaining beam property and improve COD threshold. The tapered waveguide not only enhances the output power, but also helps achieve wavelength stabilization due to current distribution. Our device weakens the trade-off among SLM, high output power and high beam quality of semiconductor lasers. Further study would focus on optimizing structural parameters to improve the performance of the device.

4. Conclusion

The SLM, high-power, fundamental transverse mode regrowth-free gain-coupled DFB laser based on the periodic current injection from periodic surface p-contacts with simple micrometer-scale

fabrication technology by standard i-line lithography has been demonstrated at 990 nm. Thanks to the gain-coupled DFB ridge waveguide combined with a tapered waveguide, the CW output power of the device reaches up to 0.681 W at 3 A. The slop efficiency is up to 0.27 W/A, twice larger than 0.11 W/A of the previously reported lasers [25]. The maximum output power in SLM operation is 0.303 W at 1.4 A, much larger than reported high power SLM lasers [1]. High SMSR is over 35 dB, larger than diode lasers with nanometer-scale gratings [26]. Narrow 3 dB linewidth of 1.41 pm is much narrower than laser with surface high-order gratings [2]. The far field divergence angle in the slow axis is only 15.05°, the beam quality factor M^2 in the slow axis is 1.245, achieving a laterally near-diffraction-limit emission, and is better than previously published SLM DFB lasers [30]. Due to the excellent electro-optical, spectral and spatial properties, our device provides a practical low-cost method to realize high-power, narrow-linewidth, SLM laser. High beam quality with fundamental transverse mode at high output power is especially desirable for beam shaping and coupling, and our device is extremely attractive for mass production in widespread commercial applications. Since the output power and the beam quality of the single emitter are enhanced simultaneously, the laser bars, stacks and modules will receive a good chance of development in more use areas.

References

[1] S. Spiebberger, M. Schiemangk, A. Wicht, H. Wenzel, O. Brox, and G. Erbert, "Narrow linewidth DFB lasers emitting near a wavelength of 1064 nm," *J. Lightw. Technol.,* vol. 28, no. 17, pp. 2611–2616, Sep. 2010.

[2] T. N. Vu, A. Klehr, B. Sumpf, H. Wenzel, G. Erbert, and G. Trankle, "Tunable 975 nm nanosecond diode-laser-based master-oscillator power-amplifier system with 16.3 W peak power and narrow spectral linewidth below 10 pm," *Opt. Lett.*, vol. 39, no. 17, pp. 5138–5141, 2014.

[3] L. Greusard and D. Costantini, "Near-field analysis of metallic DFB lasers at telecom wavelengths," *Opt. Exp.*, vol. 21, pp. 10422–10429, 2013.

[4] W. Schulz and R. Poprawe, "Manufacturing with novel high-power diode lasers," *IEEE J. Sel. Top. Quantum Electron*, vol. 6, pp. 696–705, Jul./Aug. 2000.

[5] H. Jeon, J. M. Verdiell, M. Ziari, and A. Mathur, "High-power low-divergence semiconductor lasers for GaAs-based 980-nm and InP-based 1550-nm applications," *IEEE J. Sel. Topics Quantum Electron.*, vol. 3, no. 6, pp. 1344–1350, Dec. 1998.

[6] R. R. Alfano and A. G. Doukas, "Introduction to the special issue on lasers in biology and medicine," *IEEE J. Quantum Electron.*, vol. 20, no. 12, p. 1342, 1984.

[7] B. W. Tilma *et al.*, "Recent advances in ultrafast semiconductor disk lasers," *Light Sci. Appl.*, vol. 4, no. 7, 2015, Art. no. e310.

[8] E. C. Burrows and K. Y. Liou, "High resolution laser LIDAR utilising two-section distributed feedback semiconductor laser as a coherent source," *Electron. Lett.*, vol. 26, no. 9, pp. 577–579, 1990.

[9] A. R. Nehrir, K. S. Repasky, and J. L. Carlsten, "Eye-safe diode-laser-based micropulse differential absorption lidar (DIAL) for water vapor profiling in the lower troposphere," *J. Atmos. Ocean. Technol.*, vol. 28, no. 2, pp. 131–147, 2011.

[10] J. Fricke *et al.*, "Properties and fabrication of high-order bragg gratings for wavelength stabilization of diode lasers," *Semicond. Sci. Technol.*, vol. 27, no. 27, 2012, Art. no. 055009.

[11] G. A. Sanders *et al.*, "Development of compact resonator fiber optic gyroscopes," in *Proc. IEEE Int. Symp. Inertial Sensors Syst. (INERTIAL)*, 2017, pp. 168–170.

[12] H. Kogelnik and C. V. Shank, "Coupled-wave theory of distributed feedback lasers," *J. Appl. Phys.*, vol. 43, no. 5, pp. 2327–2335, 1972.

[13] F. Gao *et al.*, "Study of gain-coupled distributed feedback laser based on high order surface gain-coupled gratings," *Opt. Commun.*, vol. 410,, pp. 936–940, 2018.

[14] S. R. Chinn, "Effects of mirror reflectivity in a distributed-feedback laser," *IEEE J. Quantum Electron.* vol. 9, no. 6, pp. 574–580, Jun. 1973.

[15] H. Soda, Y. Kotaki, H. Sudo, and H. Ishikawa, "Stability in single longitudinal mode operation in GaInAsP/InP phase adjusted DFB lasers," *IEEE J. Quantum Electron.*, vol. 23, no. 6, pp. 804–814, Jun. 1987.

[16] J. Li *et al.*, "Experimental demonstration of distributed feedback semiconductor lasers based on reconstruction equivalent-chirp technology," *Opt. Exp.*, vol. 17, no. 7, pp. 5240–5245, 2009.

[17] Y. Shi, S. Li, R. Guo, R. Liu, Y. Zhou, and X. Chen, "A novel concavely apodized DFB semiconductor laser using common holographic exposure," *Opt. Exp.*, vol. 21, no. 13, pp. 16022–16028, 2013.

[18] S. Nilsson, T. Kjellberg, T. Klinga, R. Schatz, J. Wallin, and K. Streubel, "Improved spectral characteristics of MQW-DFB lasers by incorporation of multiple phase-shifts," *J. Lightw. Technol.*, vol. 13, no. 3, pp. 434–441, Mar. 1995.

[19] Y. Luo, Y. Nakano, K. Tada, T. Inoue, H. Hosomatsu, and H. Iwaoka, "Purely gain-coupled distributed feedback semiconductor laser," *Appl. Phys. Lett.*, vol. 56, no. 17, pp. 1620–1622, 1990.

[20] A. Orth, J. P. Reithmaier, R. Zeh, H. Doleschel, and A. Forchel, "First order gain-coupled GaInAs/GaAs distributed feedback laser diodes patterned by focused ion beam implantation," *Appl. Phys. Lett.*, vol. 69, no. 13, pp. 1906–1908, 1996.

[21] Y. Nakano, Y. Luo, and K. Tada, "Facet reflection independent, single longitudinal mode oscillation in a GaAlAs/GaAs distributed feedback laser equipped with a gain coupling mechanism," *Appl. Phys. Lett.*, vol. 55, no. 16, pp. 1606–1608, 1989.
[22] A. Müller *et al.*, "DBR tapered diode laser with 12.7 W output power and nearly diffraction-limited, narrowband emission at 1030 nm," *Appl. Phys.*, vol. 122, p. 87, 2016.
[23] S. Sujecki and L. Borruel, "Nonlinear properties of tapered laser cavities," in *IEEE J. sel. topics quantum electronic*, vol. 9, no. 3, pp. 823–834, 2003.
[24] F. Gao *et al.*, "Two-segment gain-coupled distributed feedback laser," *IEEE Photon. J.*, vol. 10, no. 1, Feb. 2018, Art. no. 1500509.
[25] T. W. Johannes, A. Rast, W. Harth, and J. Rieger, "Gain-coupled DFB lasers with a titanium surface bragg grating," *Electron. Lett.*, vol. 31, no. 5, pp. 370–371, 2002.
[26] L. Liu, H. Qu, Y. Wang, Y. Liu, Y. Zhang, and W. Zheng, "High-brightness single-mode double-tapered laser diodes with laterally coupled high-order surface grating," in *Opt. Lett.*, vol. 39, no. 11, pp. 3231–3234, 2014.
[27] F. Gao *et al.*, "Narrow-strip single-longitudinal-mode laser based on periodic anodes defined by i-line lithography," *IEEE Photon. J.*, vol. 10, no. 2, Apr. 2018, Art. no. 1501910.
[28] Y. Chen *et al.*, "Gain-coupled distributed feedback laser based on periodic surface anode canals," *Appl. Opt.*, vol. 82, no. 10, pp. 8863–8866, 2015.
[29] S. L. Chuang, *Physics of Photonic Devices*, Berlin, Germany: Wiley, 2009.
[30] M. Mikulla, "Tapered high-power, high-brightness diode lasers: Design and performance," in *Topics Appl. Phys.*, vol. 78, pp. 265–288, 2000.
[31] S. F. Yu, "Double-tapered-waveguide distributed feedback lasers for high-power single-mode operation." in *IEEE J. Quantum Electronics*, vol. 33, no. 1, pp. 71–80, Jan. 1997.